

Accumulation of partly folded states in the equilibrium unfolding of the pneumococcal choline-binding module C-LytA

Beatriz MAESTRO and Jesús M. SANZ¹

Instituto de Biología Molecular y Celular, Universidad Miguel Hernández, Av. Universidad, s/n, E-03202 Elche (Alicante), Spain

Choline-binding modules are present in some virulence factors and many other proteins of *Streptococcus pneumoniae* (Pneumococcus). The most extensively studied choline-binding module is C-LytA, the C-terminal moiety of the pneumococcal cell-wall amidase LytA. The three-dimensional structure of C-LytA is built up from six loop-hairpin structures forming a left-handed β -solenoid with four choline-binding sites. The affinity of C-LytA for choline and other structural analogues allows its use as an efficient fusion tag for single-step purification of hybrid proteins. In the present study, we characterize the folding and stability of C-LytA by chemical and thermal equilibrium denaturation experiments. Unfolding experiments using guanidinium chloride at pH 7.0 and 20°C suggest the existence of two partly folded states (I_1 and I_2) in the following model: N (native) \rightarrow $I_1 \rightleftharpoons I_2$. The N \rightarrow I_1 transition is non-co-operative and irreversible, and is significant even in the absence of a denaturant. In contrast, the $I_1 \rightleftharpoons I_2$

transition is co-operative and reversible, with an associated free-energy change (ΔG^0) of $30.9 \pm 0.8 \text{ kJ} \cdot \text{mol}^{-1}$. The residual structure in the I_2 state is unusually stable even in 7.4 M guanidinium chloride. Binding of choline stabilizes the structure of the native state, induces its dimerization and prevents the accumulation of the I_1 species ($[N]_2 \rightleftharpoons [I_2]_2$, $\Delta G^0 = 50.1 \pm 0.8 \text{ kJ} \cdot \text{mol}^{-1}$). Fluorescence and CD measurements, gel-filtration chromatography and limited proteolysis suggest that I_1 differs from N in the local unfolding of the N-terminal β -hairpins, and that I_2 has a residual structure in the C-terminal region. Thermal denaturation of C-LytA suggests the accumulation of at least the I_1 species. These results might pave the way for an effective improvement of its biotechnological applications by protein engineering.

Key words: affinity tag, choline-binding module, C-LytA, partly folded state, protein folding, β -solenoid.

INTRODUCTION

LytA amidase, the major murein hydrolase from *Streptococcus pneumoniae*, catalyses the cleavage of the *N*-acetylmuramoyl-L-alanine bond of the peptidoglycan backbone [1]. It is involved in the separation of the daughter cells at the end of cell division [2] and in cellular autolysis, where it mediates the release of toxins that damage the host tissues and allows the entry of pneumococcal cells, leading to pneumonia, meningitis or bacteraemia [3–5]. LytA activity is strongly dependent on the presence of choline residues in the teichoic acids of the cell wall of this bacterium. Genetic and biochemical experiments have shown that the enzyme consists of two modules: a so-called ChBD (choline-binding domain) at the C-terminus, which anchors the enzyme to the cell wall through the specific recognition of choline, and an N-terminal domain housing the active site for catalysis [6–8]. Such a modular organization is also observed in other proteins [9] (see Pfam ID code PF01473; <http://www.sanger.ac.uk/Software/Pfam/index.shtml>).

The C-LytA (C-terminal module of LytA) is the major representative of the ChBD family. It is composed of six tandem ChBRs (choline-binding repeats), each composed of approx. 20 amino acids. The crystal structure of choline-ligated C-LytA reveals a novel left-handed $\beta\beta\beta$ -solenoid fold formed by the stacking of six loop- β -hairpin structures, corresponding to the ChBR, into an elongated left-handed superhelix [10, 11] (Figure 1). Four choline-binding sites are located between two consecutive ChBRs. Each choline-binding site comprises three aromatic residues, from two consecutive hairpins with the contribution of an additional hydrophobic side chain. The ligand is bound and stabilized probably by hydrophobic and cation- π interactions. Calorimetric and spectroscopic analyses have demonstrated the presence of low-affinity

and high-affinity choline-binding sites [12, 13]. Binding of choline promotes dimerization through the stacking of ChBR6 [10] and confers stability to C-LytA against thermal denaturation [12, 13], probably by shielding the otherwise solvent-exposed hydrophobic patches between ChBRs [10]. The structure of the ligand-free protein is not yet available. Although the use of NMR spectroscopy would be extremely valuable in obtaining structural data of C-LytA, the application of this technique is complicated by the poor solubility of the protein together with the dimerization process that takes place at high concentrations even in the absence of choline [13].

Structural studies of C-LytA are of interest for several reasons. Little is known about the folding and stability of β -solenoids like C-LytA [12, 13]. Moreover, LytA amidase takes part in severe pathological processes (see above). Therefore a detailed knowledge of its structure and folding could aid in the rational design of inhibitors of this and other related peptidoglycan hydrolases containing ChBDs that might be of therapeutic interest. Finally, a current application of C-LytA is based on exploiting its affinity for choline and choline analogues [14], leading to the development of a system of single-step chromatographic immobilization and purification of hybrid proteins containing this ChBD ([15, 17–19], and C-LYTAG[®] Purification System User's Manual from Biomedal, <http://www.biomedal.es>). Therefore studies on the folding of this polypeptide could then be used to rationally modify and optimize this affinity-based chromatographic system.

To gain a deeper insight into the folding of C-LytA, we have focused our attention on the chemical denaturation of the protein at 20°C and pH 7.0 and the role of its ligand, choline, using a combination of approaches. Our results suggest the accumulation of two partly folded states, I_1 and I_2 , in the presence of GdmCl

Abbreviations used: ANS, 8-anilino-naphthalene-1-sulphonic acid; ChBD, choline-binding domain; ChBR, choline-binding repeat; DSC, differential scanning calorimetry; GdmCl, guanidinium chloride; GdmSCN, guanidinium thiocyanate.

¹ To whom correspondence should be addressed (email jmsanz@umh.es).

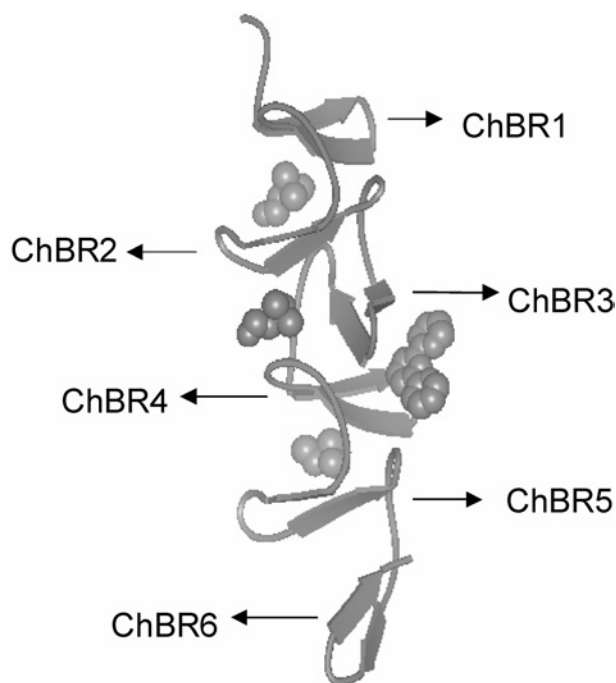


Figure 1 Structure of choline-bound C-LytA and ChBRs

Only one chain of the dimer is shown. Choline residues are displayed as van der Waals spheres. The binding site located between ChBR3 and ChBR4 is occupied in the crystal by (2,2'-6',2''-terpyridine)-platinum II¹⁰.

(guanidinium chloride), and the persistence of residual native-like structure in the I₂ species at the highest concentration of denaturant. Moreover, we propose the identification of the I₁ species with another intermediate that accumulates on heat denaturation [13]. Finally, we discuss the possible application of these results to improve the biotechnological potential of C-LytA.

EXPERIMENTAL

Materials

GdmCl, GdmSCN (guanidinium thiocyanate) and potassium dichromate were purchased from VWR International Eurolab (Mollet del Valles, Spain). ANS (8-anilinonaphthalene-1-sulphonic acid) was obtained from Sigma–Aldrich (Madrid, Spain). Choline chloride, trypsin, chymotrypsin, Dextran Blue and DEAE-cellulose were from Sigma. Owing to the hygroscopic properties of choline, concentrated stock solutions were always prepared from a freshly opened bottle and stored in aliquots at -20°C .

Protein purification

C-LytA was purified by affinity chromatography from the over-producing *Escherichia coli* strain RB791 [pCE17] as described previously [7]. Purified protein was subsequently dialysed at 20°C against 20 mM sodium phosphate buffer (pH 7.0) plus 50 mM NaCl to remove the bound choline. Dialysis performed at 4°C resulted in reversible precipitation of the protein inside the dialysis bag, especially when the sample was concentrated. Protein concentration was determined spectrophotometrically as described previously [7] using a molar absorption coefficient at 280 nm of $62\,540\ \text{M}^{-1}\cdot\text{cm}^{-1}$.

CD spectroscopy

CD experiments were performed in a Jasco J-810 spectropolarimeter fitted with a thermostatically controlled cell holder and

interfaced with a Neslab RTE-111 water bath. Isothermal wavelength spectra were acquired at a scan speed of $50\ \text{nm}\cdot\text{min}^{-1}$ with a response time of 2 s and averaged over at least six scans at 20°C . Protein concentration was $6.3\ \mu\text{M}$ and the cuvette path length was 1 or 2 mm. For GdmCl titrations, aliquots from an 8.0 M denaturant stock solution were added stepwise and incubated for 5 min before recording the wavelength spectra. Ellipticities ($[\theta]$) are expressed in units of $\text{degrees}\cdot\text{cm}^2\cdot\text{dmol}^{-1}$, using the residue concentration of the protein. With GdmCl present, spectra could not be recorded below 215 nm, due to the high absorbance of the sample.

CD-monitored thermal denaturation experiments were performed in a 1 mm path cell. The sample was layered with mineral oil to avoid evaporation, and the heating rate was $60^{\circ}\text{C}\cdot\text{h}^{-1}$. When a second scan was required, the heated sample was cooled down in the same cuvette and left for low-temperature equilibration for at least 1 h.

Fluorescence spectroscopy

Fluorescence measurements were performed on an Aminco SLM8000 spectrofluorimeter using a $5\ \text{mm}\times 5\ \text{mm}$ path-length cuvette and a protein concentration of $6.3\ \mu\text{M}$. Tryptophan emission spectra were obtained using an excitation wavelength of 280 nm, with excitation and emission slits of 4 nm and a scan rate of $60\ \text{nm}\cdot\text{min}^{-1}$. We monitored the ratio of intensities at 325 and 365 nm to avoid errors caused by slight changes in protein concentration. For GdmCl or GdmSCN titrations, aliquots from an 8.0 M denaturant stock solution were added stepwise and incubated for 5 min before starting measurements. ANS fluorescence spectra were recorded on excitation of the probe at 380 nm and emission was registered between 400 and 600 nm, using excitation and emission slits of 4 nm and a scan rate of $60\ \text{nm}\cdot\text{min}^{-1}$. Final ANS concentration was 0.1 mM.

Data analysis

Equilibrium unfolding was fitted by the method of least squares to the corresponding two-state process according to eqn (1) [20]:

$$\Delta G = \Delta G^0 - m [\text{denaturant}] \quad (1)$$

where ΔG and ΔG^0 are the free energies of unfolding in the presence and absence of denaturant respectively and m represents the dependence of ΔG with respect to [denaturant].

Size-exclusion chromatography

Samples of $65\ \mu\text{l}$ containing $200\ \mu\text{g}$ of C-LytA were loaded on to a Sephadex G-75 column ($26\ \text{cm}\times 0.9\ \text{cm}$) (Sigma) or a Toyopearl HW-55F column ($50\ \text{cm}\times 2.5\ \text{cm}$) (Tosoh, Tokyo, Japan) equilibrated in 20 mM sodium phosphate buffer (pH 7.0) plus 200 mM NaCl for different GdmCl and/or choline concentrations, and were run with the same buffer at a flow rate of $0.5\ \text{ml}\cdot\text{min}^{-1}$ at 20°C . Fractions of $500\ \mu\text{l}$ were collected and their absorbance was measured at 280 nm. Exclusion (6.3 ml for Sephadex, 28.6 ml for Toyopearl) and total (21.0 ml for Sephadex, 68.0 ml for Toyopearl) volumes were determined with Dextran Blue and potassium dichromate respectively.

Limited proteolysis

Trypsin and chymotrypsin digestion of C-LytA ($0.3\ \text{mg}\cdot\text{ml}^{-1}$) was performed at 25°C in 20 mM phosphate buffer (pH 8.0) using a 1:50 (w/w) protease/protein ratio. Aliquots were withdrawn at different times and the reaction was stopped by the addition of SDS/PAGE loading buffer [21]. Samples were stored frozen at

–20 °C until electrophoresis. Purification of the chymotrypsin-resistant C-LytA fragment [C-LytA(Δ 32)] was performed after a preparative 16 h digestion for the same protease/protein ratio. The sample was applied on to a DEAE-cellulose column and purified as described for the full-length protein. The chymotrypsin-resistant fragment was dialysed against 20 mM phosphate buffer (pH 7.0), and subsequently characterized by Edman sequencing in a 477A analyser (Applied Biosystems) and matrix-assisted laser-desorption ionization–time-of-flight MS. The laser desorption/ionization experiments were performed on a BIFLEX III time-of-flight instrument (Bruker-Franzen Analytik, Bremen, Germany) operated in the positive mode. Peptides were analysed in the reflectron mode after external calibration using myoglobin as the standard using a saturated solution of α -cyano-4-hydroxycinnamic acid in acetonitrile/water (1:2, v/v) with 0.1% trifluoroacetic acid as the matrix, and the samples were analysed in the linear mode with SA [sinapic acid (3,5-dimethoxy-4-hydroxycinnamic acid)] as the matrix. Typically, 50–100 laser shots were summed into a single mass spectrum. Equal volumes (0.5 μ l) of the sample solution and the matrix were spotted on the target and air-dried.

RESULTS

Equilibrium GdmCl titrations monitored by CD and fluorescence

The influence of GdmCl on the structure of C-LytA was first analysed by CD. It should be pointed out now that, although some specific dimerization of C-LytA may take place at neutral pH even in the absence of choline, this event is negligible at the concentrations used in our experiments (6.3 μ M), where the predominant species is the monomer (> 90%) [13]. As shown in Figure 2(A), the far-UV CD spectrum of C-LytA at pH 7.0 and 20 °C displays a maximum at 223 nm and a shoulder centred at 235 nm. This unusual spectrum does not reflect the real content of secondary structure, but accounts instead for a high contribution of aromatic side chains in the far-UV region [7, 12]. Surprisingly, we found that the CD spectrum of C-LytA under these conditions was not completely reproducible, with moderate differences in the ellipticity value and the occasional absence of the 235 nm shoulder, depending on the age of the sample and/or the number of freeze–thaw cycles. This point will be discussed below. On the other hand, addition of saturating amounts of choline (150 mM) induces a general increase in ellipticity (Figure 2A) as described before [7, 12].

The stability of C-LytA against GdmCl denaturation at pH 7.0 and 20 °C was checked by following the change in the CD signal at different GdmCl concentrations. The resulting titration curves (depicted in Figure 3A) are dependent on the wavelength observed. The $[\theta]_{219}$ value, reflecting mostly changes in secondary structure [12], decreases almost linearly up to approx. 2.0 M GdmCl, and more co-operatively at higher denaturant concentrations (Figure 3A). In contrast, the change in ellipticity at 226 nm, mainly a reporter of tryptophan environments [12], is appreciably more co-operative, with a midpoint at approx. 3.5 M GdmCl and showing no drift between 0 and 2.0 M denaturant (Figure 3A). The spectrum registered at 2.0 M GdmCl (Figure 2A) confirms a decrease in ellipticity at lower wavelengths, remaining essentially unaltered above 226 nm. These results might be indicative of the accumulation of a partly folded state at low GdmCl concentrations with some loss of secondary structure but without affecting tryptophan environments. This putative intermediate was named I_1 . On the other hand, the protein is not completely unfolded in 7.4 M GdmCl, as deduced by the presence of a broad band of positive ellipticity centred at 230 nm (Figure 2A). The spectrum

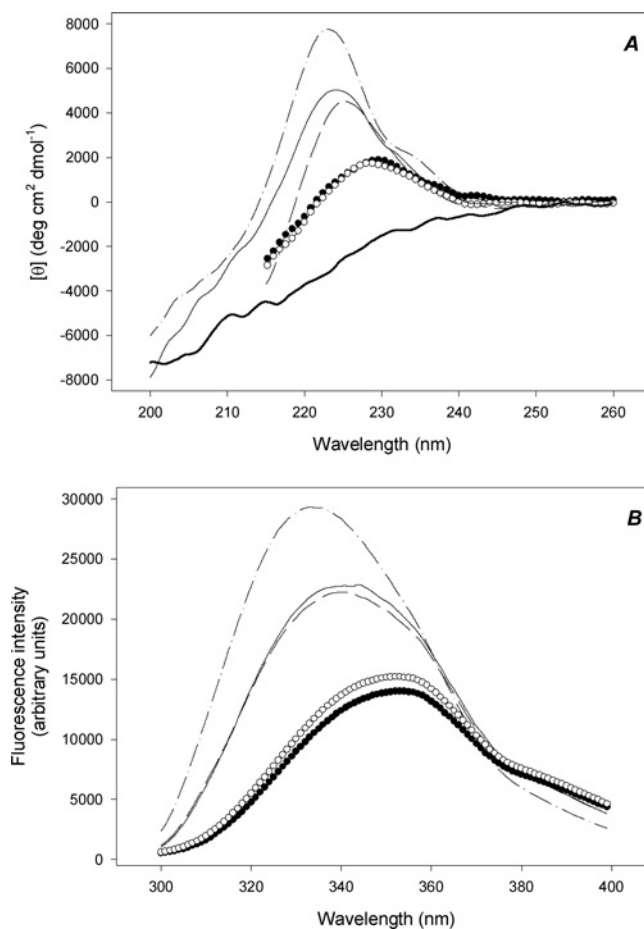


Figure 2 Spectroscopic characteristics of C-LytA

(A) Far-UV CD spectra; recorded at 20 °C in 20 mM sodium phosphate (pH 7.0) plus 0 M GdmCl (solid line), 0 M GdmCl + 150 mM choline (---), 2.0 M GdmCl (-.-.-), 7.4 M GdmCl (●), 7.4 M GdmCl + 150 mM choline (○), and in phosphate buffer at 85 °C (thick solid line). (B) Intrinsic fluorescence spectra recorded at 20 °C in 20 mM sodium phosphate (pH 7.0) in 0 M GdmCl (solid line), 0 M GdmCl + 150 mM choline (-.-.-), 2.0 M GdmCl (-.-.-), 7.4 M GdmCl (●) and 7.4 M GdmCl + 150 mM choline (○).

is very different from that of a heat-unfolded C-LytA, which shows the characteristic features of a random coil (Figure 2A). Any possible CD artifact due to the high ionic strength provided by GdmCl can be ruled out, since the addition of 1.5 M NaCl to heat-unfolded C-LytA barely changes its CD spectrum (results not shown). Therefore, the residual structure remaining at high GdmCl concentrations was taken as indicative of a second, partly folded, state that was termed I_2 .

Figure 2(B) depicts the intrinsic fluorescence properties of C-LytA at 20 °C and pH 7.0. The spectrum displays a maximum at 344 nm. In the presence of 150 mM choline, the intensity of the spectrum increases and the maximum is shifted to 333 nm, reflecting the burial of the aromatic side chains involved in the binding of the ligand [10]. The change in fluorescence signal of C-LytA after GdmCl titration is also shown in Figure 3(A). The curve displays a sigmoidal shape, with a GdmCl midpoint of 3.52 M (close to that obtained on monitoring $[\theta]_{226}$), with virtually no variation in the fluorescence spectrum from 0 to 2.0 M GdmCl (populated by the I_1 species) (Figure 2B). On the other hand, in 7.4 M GdmCl, the fluorescence spectrum shows a decreased intensity and a red shift to 354 nm, reflecting the exposure of tryptophan residues to the solvent on unfolding (Figure 2B).

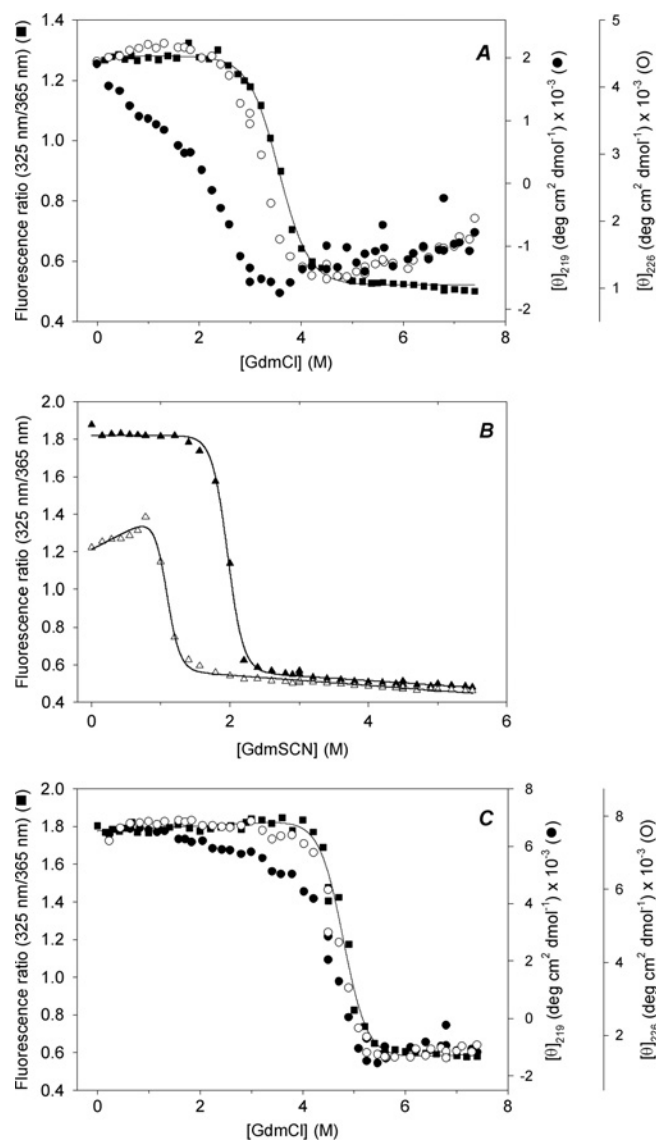


Figure 3 Stability of C-LytA against GdmCl and GdmSCN denaturation

(A) GdmCl denaturation, no additives. Unfolding was followed at 20 °C in 20 mM sodium phosphate buffer (pH 7.0) by monitoring the ellipticity signal at 219 nm (●), 226 nm (○) and the ratio of fluorescence intensities at 325 and 365 nm (■). (B) GdmSCN denaturation monitored by fluorescence, (△) without additives and (▲) in the presence of 150 mM choline. Solid lines are the fittings of fluorescence results to eqn (1). (C) GdmCl denaturation, plus 150 mM choline. Symbol scheme as in (A).

The measurement of the fluorescence of the hydrophobic probe ANS is normally used to check the presence of ‘molten globule’ states [22], i.e. conformations with near-native secondary struc-

ture but with a disrupted tertiary structure, allowing the binding of the probe to the solvent-accessible hydrophobic cores of the protein and therefore modifying its spectral features. However, we did not observe any significant binding of ANS to C-LytA at any GdmCl concentration (results not shown), suggesting that I_1 and I_2 may not be molten globule-type intermediates.

From the above experiments, it follows that two partly folded states, I_1 and I_2 , accumulate in the presence of approx. 2.0 and 7.4 M GdmCl respectively at 20 °C and pH 7.0. Other species between I_2 and the fully unfolded form cannot be detected at this temperature with this denaturant. An increase in temperature from 20 to 95 °C in the presence of 7.4 M GdmCl results in the progressive non-co-operative loss of the positive CD signal (results not shown), suggesting that the residual structure of I_2 is of decreased compactness. In an attempt to further unfold I_2 at 20 °C, a stronger denaturant such as GdmSCN was used [23]. A GdmSCN titration monitored by fluorescence spectroscopy showed a single sigmoidal transition with a midpoint of 1.1 M, followed by a linear, slightly sloping baseline up to 5.6 M denaturant (Figure 3B). This could mean that the I_2 structure persists even under these conditions, that the unfolding transition is not co-operative, or that it is barely detectable by fluorescence spectroscopy. Unfortunately, these alternatives could not be tested by CD, since a suitable CD-monitored transition could not be obtained due to the high absorbance of GdmSCN.

To check the reversibility of the unfolding transitions, a sample of C-LytA was incubated in 2.0 or 7.4 M GdmCl for 30 min and subsequently dialysed against phosphate buffer. In all the cases, the resulting CD spectrum turned out to be fully coincident with the spectrum recorded at 2.0 M GdmCl, i.e. that corresponding to I_1 (results not shown). Moreover, accumulation of I_1 may also occur under non-denaturing conditions, with aged or repeatedly freeze–thawed samples explaining the lack of reproducibility of the native CD spectrum described above. In accordance with this, the fact that the $[\theta]_{219}$ titration within the 0–2.0 M GdmCl range is linear and shows no pre-transitional baseline strongly suggests the existence of a pre-established $N \rightarrow I_1$ transition which is very sensitive to low denaturant concentrations.

The results shown so far suggest that the $N \rightarrow I_1$ transition is non-co-operative and essentially irreversible in the absence of choline, involving the unfolding of a part of C-LytA that either involves solvent-exposed tryptophans or lacks these residues. This would explain why the $N \rightarrow I_1$ transition is not detected by Trp fluorescence or by $[\theta]_{226}$. Assuming that the co-operative curve observed by fluorescence reports the $I_1 \rightleftharpoons I_2$ equilibrium without interference from the $N \rightarrow I_1$ transition, fluorescence results were fitted into a two-state unfolding equation using the linear extrapolation model (eqn 1). Results of the fitting are shown in Figure 3(A) and Table 1, with a calculated free energy of unfolding in the absence of denaturant [ΔG^0 of $(30.9 \pm 0.8) \text{ kJ} \cdot \text{mol}^{-1}$]. Results obtained with GdmSCN (Figure 3B) yielded similar ΔG^0 values [$(28.4 \pm 2.1) \text{ kJ} \cdot \text{mol}^{-1}$], although the fits are characterized by larger errors, especially in the m value (Table 1).

Table 1 Thermodynamic quantities of the equilibrium denaturation of C-LytA

Results were calculated using eqn (1). Results are the average of at least three experiments. Choline-saturated species are represented as ‘ch’.

Protein	Denaturant	m ($\text{kJ} \cdot \text{mol}^{-1} \cdot \text{M}^{-1}$)	[Denaturant] $_{1/2}$ (M)	Transition	ΔG^0 ($\text{kJ} \cdot \text{mol}^{-1}$)
Native	GdmCl	8.8 ± 0.4	3.5 ± 0.1	$I_1 \rightleftharpoons I_2$	30.9 ± 0.8
Native	GdmSCN	25.9 ± 2.1	1.1 ± 0.1	$I_1 \rightleftharpoons I_2$	28.4 ± 2.1
Native + choline (150 mM)	GdmCl	10.4 ± 0.8	4.8 ± 0.1	$N_2 \cdot \text{ch} \rightleftharpoons (I_2)_2 \cdot \text{ch}$	50.1 ± 0.8
Native + choline (150 mM)	GdmSCN	21.7 ± 1.3	2.0 ± 0.1	$N_2 \cdot \text{ch} \rightleftharpoons (I_2)_2 \cdot \text{ch}$	43.5 ± 1.3

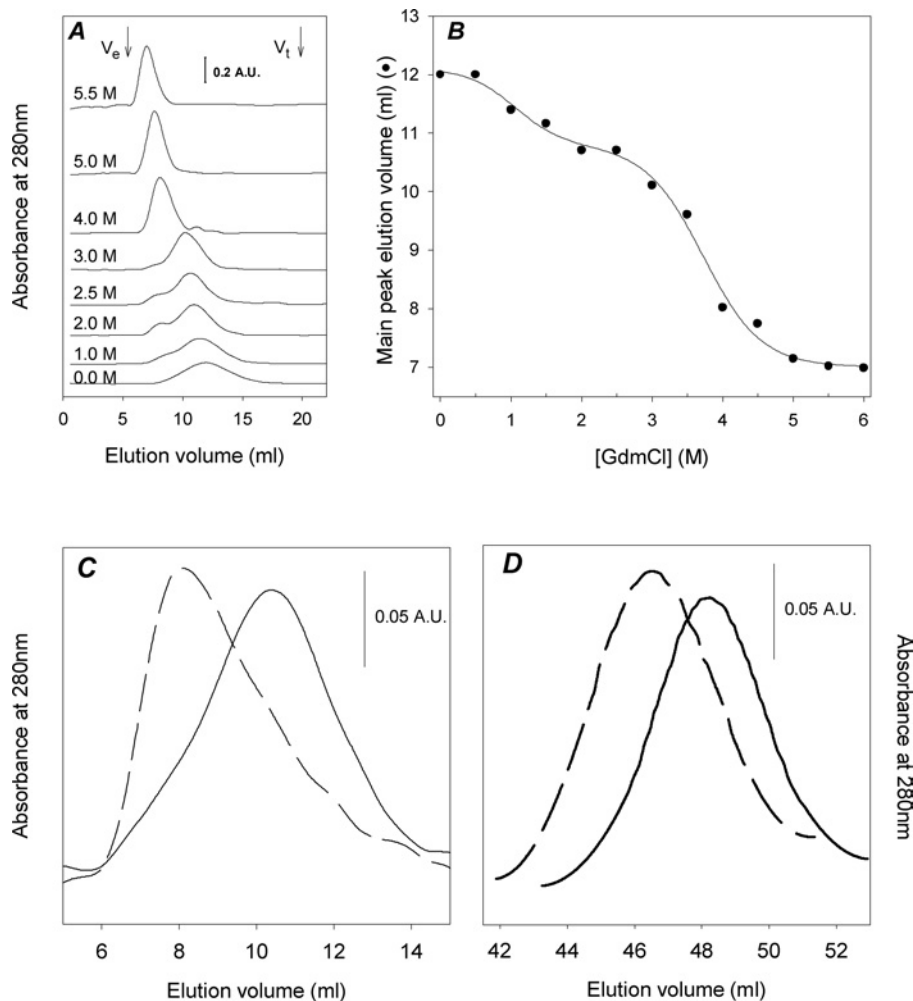


Figure 4 Size-exclusion chromatography of C-LytA

(A) UV-absorption profiles registered in a Sephadex G-75 column at several GdmCl concentrations. V_e and V_t are the exclusion and total volumes of the column respectively. A.U., absorbance units. The curves are shifted along the Y-axis for clarity of presentation. Only one set of experiments is shown, in which a secondary peak is evident between 1.0 and 3.0 M GdmCl. (B) Plot of the elution volume of the main peak corresponding to the profiles shown in (A). Results are the average of three experiments. The solid line is drawn only for presentation purposes. (C) A comparison of the elution profiles of C-LytA in the presence of 2.0 M GdmCl (solid line) and 2.0 M GdmCl + 3.0 mM choline (dashed line). (D) A comparison of the elution profiles of C-LytA in a Toyopearl HW-55F column in the presence of 6.0 M GdmCl (thick solid line) and 6.0 M GdmCl + 150 mM choline (thick dashed line).

Effect of choline on unfolding

Figure 3(C) shows the GdmCl-induced unfolding curves of C-LytA in the presence of 150 mM choline, a concentration sufficient to saturate all the choline-binding sites [13]. In this case, the initial drift of the $[\theta]_{219}$ signal was drastically reduced and, as a consequence, the CD denaturation curves were nearly independent of the wavelength monitored and virtually coincident with the fluorescence titration. A significant increase in the $[\theta]_{226}$ transition midpoint is evident (4.70 M). The GdmCl denaturation turned out to be completely reversible on dialysis of the denaturant, while keeping the choline concentration as 150 mM (results not shown). The final conformational state accumulated at 7.4 M GdmCl displays a CD spectrum that is superimposable with that of I_2 (Figure 2A). These results would indicate the relative destabilization of I_1 , so that unfolding proceeds mostly from the dimeric native state to the I_2 species following an apparent two-state transition. The fact that the fluorescence spectrum recorded at 7.4 M GdmCl plus 150 mM choline displays a modest (10%) but very reproducible increase in intensity (not ascribed to experimental error) when compared with that of the unligated

form (Figure 2B) suggests that the residual structure in the I_2 state is able to retain some ligand molecules bound to it.

Size-exclusion chromatography

This technique provides information on the overall shape of polypeptides, and has been usually employed to track the equilibrium unfolding of proteins [24]. Figure 4(A) shows the elution profile of C-LytA in a Sephadex G-75 column at pH 7.0 and 20 °C equilibrated in different GdmCl concentrations. Experiments could not be performed at denaturant concentrations higher than 5.6 M due to severe flow restrictions in the column. In the absence of a denaturant, C-LytA is eluted as a single broad peak. It should be mentioned here that gel-filtration chromatography is not useful to obtain information about the molecular mass of C-LytA, as described before [25], probably due to the non-globular elongated shape of the protein [10]. On increasing the concentration of GdmCl, the elution peak shifts to lower volumes, in accordance with a concomitant higher proportion of extended molecules. Interestingly, we observed, in some cases, a minor peak centred at a lower volume in the range between 1.0 and 3.0 M GdmCl

(Figure 4A), whereas in other assays this additional peak was not evident (e.g. Figure 4C). A plot of the elution volume of the main peak against GdmCl concentration unveils a clear biphasic transition (Figure 4B). There is a shallow change between 0 and 2.0 M GdmCl followed by a second, more co-operative, transition, the midpoint of which is 3.70 M. This value is comparable with the denaturation midpoint calculated by fluorescence spectroscopy (3.52 M, Table 1), suggesting that both techniques are monitoring the same event. The first transition may be related to the low-co-operative change detected by $[\theta]_{219}$ at low GdmCl concentrations (Figure 3A). These results are in agreement with a partial unfolding of C-LytA between 0 and 2.0 M GdmCl to form an extended I_1 species, which subsequently converts it into a more expanded I_2 at higher denaturant concentrations.

Limited proteolysis

Our results show that the accumulation of I_1 in the absence of choline can be achieved either spontaneously or under mild denaturing conditions (2.0 M GdmCl). Therefore the stability of the region of the protein that is unfolded in I_1 must be low when compared with the rest of the protein and probably more accessible to proteases. In an attempt to further characterize this intermediate, a limited proteolysis experiment was performed on C-LytA using trypsin and chymotrypsin at 20°C. Whereas the protein is fairly resistant to trypsin under these conditions (results not shown), a chymotrypsin digest yielded a stable core fragment after a 16 h incubation (Figure 5, top panel), which was further purified by affinity chromatography on DEAE-cellulose (see the Experimental section above). Five cycles of Edman degradation yielded the sequence MLADR, coincident with residues 33–37 of the full-length protein. This demonstrates that there is a site especially accessible to chymotrypsin in the middle of the loop corresponding to the ChBR2 (Figure 1), giving rise to a fragment of theoretical mass 12 197.3 Da. This is in accordance with an MS analysis of the fragment that indicated a molecular mass of 12 209.8 Da. The proteolytic-resistant species was named C-LytA(Δ 32). The fact that C-LytA(Δ 32) could be purified on DEAE-cellulose suggests that its overall affinity to choline and DEAE is comparable with the full-length protein despite the loss of one and a half ChBRs.

The purified C-LytA(Δ 32) was characterized by CD spectroscopy. The far-UV CD spectrum of the C-LytA(Δ 32) is remarkably similar to that of I_1 (Figure 5, middle panel). Moreover, a GdmCl titration of C-LytA(Δ 32) followed by $[\theta]_{219}$ lacks the characteristic low-co-operativity decrease in the signal up to 2.0 M assigned to the $N \rightarrow I_1$ transition, but preserves the co-operative change ascribed to the $I_1 \rightleftharpoons I_2$ equilibrium as monitored by $[\theta]_{226}$ (Figure 5, bottom panel). These results strongly suggest that C-LytA(Δ 32) may represent the I_1 species, and therefore points to the unfolding of the N-terminal part of C-LytA as leading to the accumulation of this state.

Effect of low choline concentration on the unfolding equilibria

The three-dimensional structure of choline-saturated C-LytA reveals that the C-terminal repeat (ChBR6) is atypical with respect to the others, as it lacks tryptophans, its position deviates from the solenoid axis and constitutes the choline-induced dimerization surface [10,11]. In the monomeric form (i.e. with choline absent), this hairpin may have few tertiary contacts with the rest of the molecule and so would be only marginally stable. It could therefore be another candidate for that part of the protein that unfolds in the $N \rightarrow I_1$ transition. This hypothesis is consistent with the unfolding being insensitive to Trp fluorescence or $[\theta]_{226}$ measure-

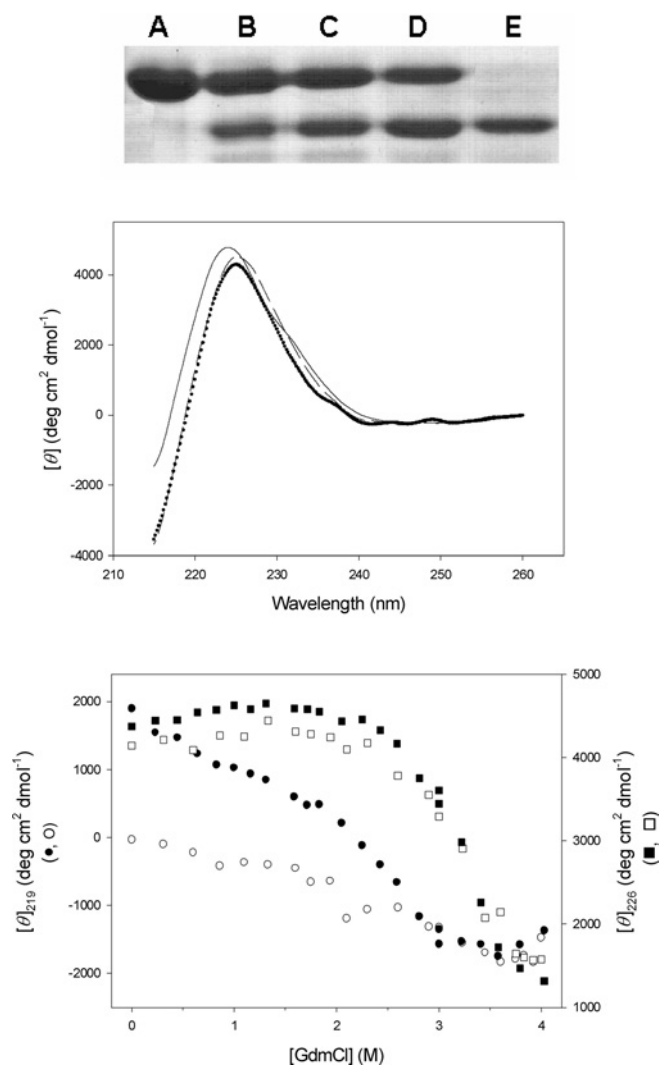


Figure 5 Chymotrypsin digestion of C-LytA

Top panel, SDS/PAGE analysis. Lanes A–E show samples taken at 0, 30, 60 and 120 min and 16 h respectively; Middle panel, far-UV CD spectra of native C-LytA (—), of C-LytA in phosphate buffer plus 2.0 M GdmCl (---) and of C-LytA(Δ 32) (· · · · ·); Bottom panel, CD-monitored GdmCl titration of C-LytA (filled symbols) and of C-LytA (Δ 32) (open symbols) at 219 nm (circles) and 226 nm (squares).

ments as this part is tryptophan-deficient, but contrasts with the results from limited proteolysis discussed above. To decide between these possibilities, we performed fluorescence- and CD-monitored GdmCl unfolding titrations at low concentrations of choline (1.5 and 3.0 mM), where the occupation of the high-affinity-binding sites takes place exclusively [13]. This induces dimerization (up to 75 and 90% respectively [13]) that should stabilize the ChBR6 against GdmCl denaturation. Since the ellipticity of C-LytA in the absence of additives is variable depending on the age of the sample (see above), we performed a control experiment on the same day using the same batch of protein but without choline. As depicted in Figure 6(A), the curves obtained by plotting $[\theta]_{226}$ are almost superimposable in all three cases (0, 1.5 and 3.0 mM choline), together with a fluorescence titration performed in 3.0 mM choline. In contrast, substantial differences are seen at 219 nm (Figure 6B). In this case, the linear loss of ellipticity before the main co-operative change presents an enhanced amplitude on the addition of 1.5 and 3.0 mM choline,

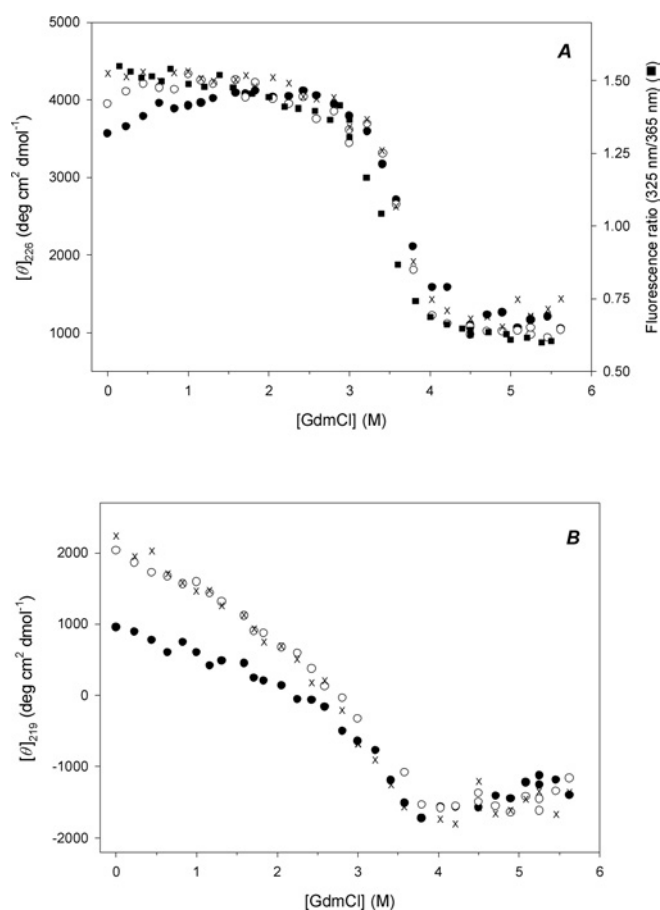


Figure 6 GdmCl denaturation of C-LytA at low choline concentration

The far-UV CD signal was followed at 226 nm (A) and 219 nm (B), in the absence of choline (●), in 1.5 mM choline (×) and in 3.0 mM choline (○). A fluorescence-monitored titration at 3.0 mM choline (■) is also overlaid in (A).

although it still takes place within approximately the same GdmCl range as in the absence of ligand. This suggests that binding of high-affinity choline does not change the observed unfolding scheme of unligated C-LytA, that is, it does not preclude the accumulation of I_1 even though the ChBR6 motif involved in dimerization is stabilized. The augmented amplitude ascribed to the $N \rightarrow I_1$ change is in accord with the increase in calorimetric enthalpy of the low-temperature endotherm observed by DSC (differential scanning calorimetry) at low choline concentration [13] (see below), which was explained in terms of more molecules undergoing such a transition. On the other hand, a size-exclusion chromatography experiment performed in the presence of 3.0 mM choline and 2.0 M GdmCl showed a single broad peak centred at 8.1 ml (Figure 4C), a lower elution volume compared with the unligated I_1 (10.7 ml, Figure 4C), confirming that choline-ligated I_1 retains the dimerization state (and therefore a folded ChBR6).

Characterization of the association state of I_2

Since no significant changes are observed in the main co-operative transition ascribed to the unfolding of I_1 when compared with the situation in the absence of choline (Figure 6A), this suggests that the GdmCl-induced transitions do not affect the dimerization interface in the $I_1 \rightleftharpoons I_2$ equilibrium and that I_1 and I_2

are both dimers in the presence of choline. To verify the oligomerization state of the I_2 , we performed a size-exclusion chromatography experiment in 6 M GdmCl in the absence and presence of 150 mM choline. Owing to the expanded nature expected for the I_2 state, the more suitable Toyopearl HW-55F resin was used instead of Sephadex G-75. As shown in Figure 4(D), binding of choline to I_2 causes a significant increase in the hydrodynamic radius that is compatible with the dimerization of the protein under these conditions. Hence, assuming GdmCl does not interfere with dimerization, spectroscopic results obtained in 150 mM choline (Figure 3C) were fitted to a two-state transition between dimers [N_2 and $(I_2)_2$] (eqn 1). The associated free-energy change was calculated to be $50.1 \pm 0.8 \text{ kJ} \cdot \text{mol}^{-1} (\text{monomer})^{-1}$ (Table 1), by assuming that the regions of C-LytA undergoing the unfolding transition behave as independent co-operative units within the dimer. Similar results were obtained with GdmSCN-induced denaturation ($43.5 \pm 1.3 \text{ kJ} \cdot \text{mol}^{-1}$) (Figure 3B, Table 1).

Correspondence with thermal unfolding intermediates

DSC experiments have previously shown [13] that the thermal denaturation of C-LytA in the absence of choline involves the accumulation of two intermediates, which in the present study we refer to as I_a and I_b . The $N \rightarrow I_a$ transition is irreversible and displays a small broad peak centred at approx. 40 °C, whereas the $I_a \rightleftharpoons I_b \rightleftharpoons U$ transitions give rise to a single asymmetric peak centred at 61 °C, I_b being metastable at these temperatures. We examined the relationship between these heat-induced intermediates and those described in the present work.

Figure 7(A) shows the denaturation profile of C-LytA after increasing the temperature by monitoring the CD signal at 223 nm. This wavelength is the optimal wavelength for simultaneously following the unfolding of both secondary and tertiary structures. A first scan of a freshly purified sample displays a biphasic transition with temperature midpoints (T_m) at 43.6 ± 0.7 and 63.5 ± 0.4 °C. These values are very close to those reported from calorimetric measurements (40 and 61 °C respectively) [13], taking into account (i) that the second CD-monitored curve may comprise two overlapping transitions that can only be discerned by DSC; (ii) the necessarily higher precision of the DSC measurements and (iii) the fact that effects from any aggregation are more evident in DSC owing to the higher concentrations of protein used and tend to shift the temperature midpoints to lower values.

The CD spectrum recorded at 85 °C is characteristic of a fully unfolded protein (Figure 2A). Cooling down the sample did not restore the native CD spectrum (Figure 7B), as described before [12]. However, there are many similarities between the recovered spectrum and that of I_1 accumulated at 2.0 M GdmCl (Figure 7B). The difference in intensity may be ascribed to the irreversible aggregation of a part of the sample [13]. A second temperature scan performed on the same sample yielded virtually only the second transition [$T_m = (62.5 \pm 0.3) \text{ °C}$] (Figure 7A). These results suggest that the calorimetric I_a intermediate might correspond to the I_1 form, and that this is the predominant form of C-LytA on refolding from the heat-unfolded conformation, as also occurs with the removal of GdmCl (see above). To confirm this hypothesis, a GdmCl titration was performed at 20 °C on a protein sample previously heated up to 55 °C. As shown in Figure 7(C), the denaturation curve monitoring $[\theta]_{219}$ certainly lacks the characteristic loss of a signal up to 2.0 M assigned to the $N \rightarrow I_1$ transition. Nevertheless, the co-operative change ascribed to the $I_1 \rightleftharpoons I_2$ equilibrium is preserved as detected by $[\theta]_{226}$; although, in this case, a moderately sloping pre-transition baseline can also be seen (Figure 7C). It could be argued that the 40 °C DSC peak displays a very low intensity when compared with the 61 °C

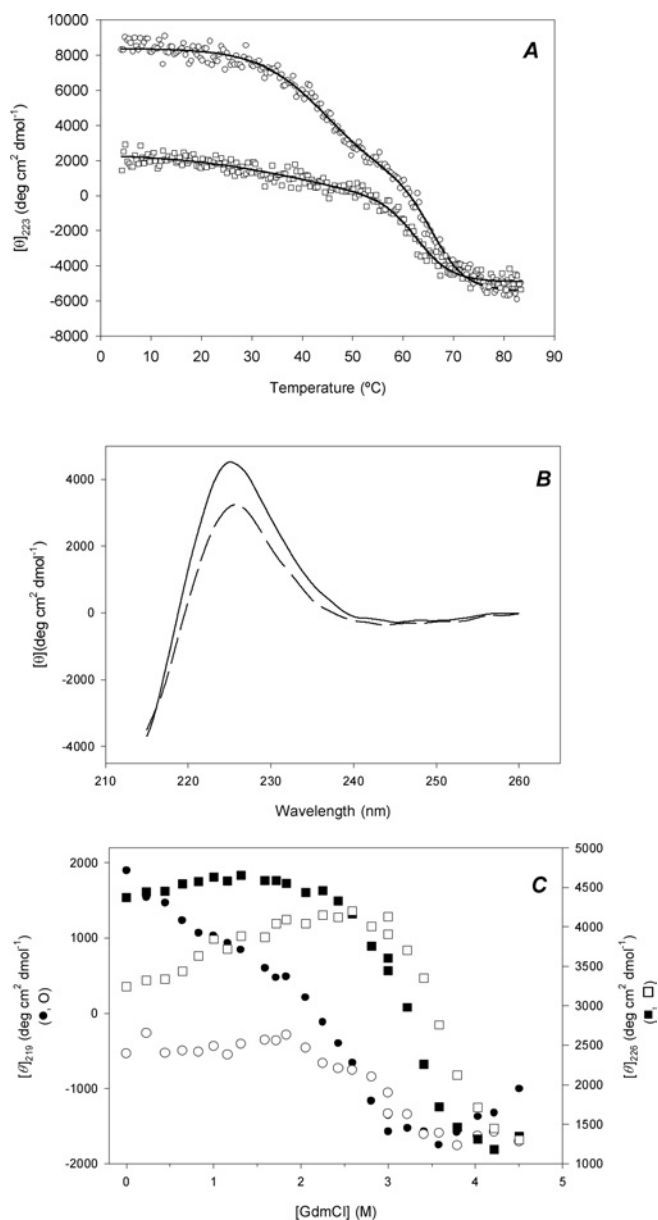


Figure 7 Correspondence of thermodynamic and thermal intermediates of C-LytA

(A) Thermal denaturation of C-LytA followed by ellipticity at 223 nm. First and second scans are represented by circles and squares respectively. Solid lines are sigmoidal fittings with no physical significance. (B) Far-UV CD spectra of C-LytA at 20 °C after a first heating scan (dashed line) and a non-heated sample in 2.0 M GdmCl (solid line). (C) CD-monitored GdmCl titration of non-heated C-LytA (filled symbols) and protein heated and cooled down (open symbols) at 219 nm (circles) and 226 nm (squares).

endotherm [13], while the two CD-monitored transitions are of comparable amplitudes (Figure 7A). However, we observed that the profiles obtained with aged samples contained a significantly decreased first transition, concomitant with our hypothesis that the native state irreversibly converts into I_1 in a slow timescale (see above). On the other hand, due to the metastability of I_b , a comparison with I_2 is not possible. Finally, it should be mentioned that on the addition of 150 mM choline, the CD-monitored thermal unfolding of C-LytA displays a single co-operative curve at higher temperatures (results not shown), in accordance with the DSC experiments [13].

DISCUSSION

ChBDs are found in many microbial enzymes that act on the rigid cell wall structure. They seem to have evolved to achieve a high-affinity, yet dynamic, mechanism of attachment to their substrate. With this, evolution might have selected the genetic concatenation of independent ChBRs for functioning rather than optimizing a single sequence with point mutations. Given this particular architecture, it would not be surprising if denaturation of ChBDs is a multistep process, arising from the independent unfolding of the ChBRs.

In the present study, we have investigated the structure and stability of the choline-binding module of the LytA amidase (C-LytA) by equilibrium denaturation experiments using GdmCl, GdmSCN and heat, in both the absence and presence of choline. To explain the complex unfolding equilibria, we propose a general scheme that is depicted in Figure 8. This scheme involves at least three structured species, the 'native' (fully folded) form (N) and two partly folded states (I_1 and I_2) that are able to dimerize with choline. The transition from N to I_1 is irreversible in the absence of a ligand (Figure 8, left path), and I_1 is the only species that accumulates on refolding of the chemical- or heat-denatured protein (Figure 7) or on storage of purified samples for more than 20 days at -20°C or overnight at room temperature (20°C). The fact that the $N \rightarrow I_1$ transition monitored by $[\theta]_{219}$ is not co-operative and lacks a defined pre-transitional baseline also suggests that C-LytA in 0 M GdmCl may already be in a partially unfolded form. Limited proteolysis experiments (Figure 5) together with denaturation experiments performed at low choline concentration (Figure 6) suggest ChBR1 and, probably, the ChBR2 motifs are the substructures in N whose unfolding results in I_1 . Since the tryptophan environments of N and I_1 are very similar (Figure 2), these residues in the N-terminal region of C-LytA must be solvent-exposed in the absence of choline. In any case, I_1 must preserve most of the C-LytA structure, since it unfolds in a co-operative manner with GdmCl (Figure 3A), GdmSCN (Figure 3B) or temperature increases (Figure 7A), with a free energy of unfolding of approx. $31 \text{ kJ} \cdot \text{mol}^{-1}$ at 20°C (Table 1). On the other hand, the residual structure at 7.4 M GdmCl (Figure 2A) is capable of interacting with choline (Figure 2B) and allows dimerization in the presence of the ligand (Figure 4D). Such structures may involve the C-terminal part of the protein, as discussed below.

Low concentrations of choline saturate the high-affinity sites in C-LytA and induce its dimerization through the binding of one molecule of ligand per monomer [13]. According to our results and on the basis of the three-dimensional structure of C-LytA, it seems reasonable to postulate (Figure 8, middle path) that at least one of these high-affinity sites is located in the vicinity of the C-terminal dimerization hairpin, i.e. between ChBRs 4 and 5 (Figure 1). In fact, the three-dimensional structure of C-LytA solved by X-ray diffraction shows the incorporation of crystallization additives that are able to replace the choline used in the purification of the protein only in the first three choline-binding sites but not in the last one [10]. Nevertheless, additional binding of choline molecules, not directly involved in dimerization, cannot be ruled out, and we propose the existence of another high-affinity site between ChBRs 1 and 2 (Figure 1). This would help to refold C-LytA molecules from I_1 to the native state, promoting the observed increase in ellipticity and in the number of molecules undergoing the $N \rightarrow I_1$ transition (Figure 6) [13]. This binding, however, would not be a sufficient contribution to stabilize against GdmCl unfolding unless the low-affinity sites are also occupied (Figure 8, right), in accordance with the suggestion of co-operativity between sites [12]. Finally, on choline saturation,

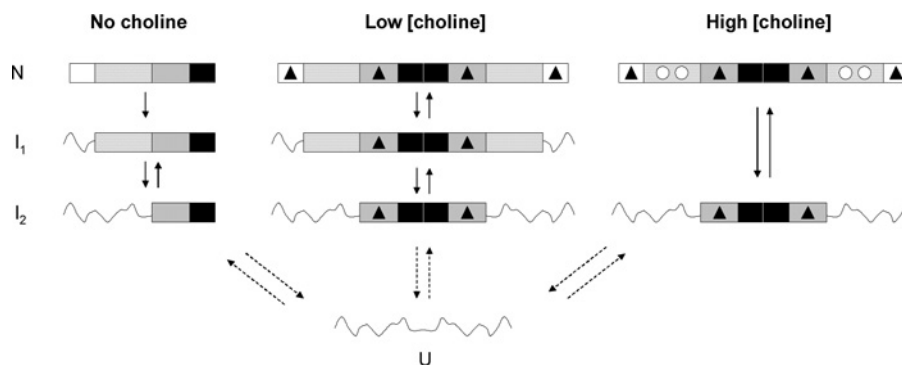


Figure 8 A proposed general scheme of C-LytA equilibrium unfolding by GdmCl

The protein is represented as a rectangle divided into structural subdomains. Unfolding of such subdomains is depicted by flexible lines. Triangles and circles represent high-affinity and low-affinity binding choline molecules respectively. The black box, without choline-binding sites, represents the dimerization subdomain ChBR6. Dashed arrows indicate equilibria that cannot be analysed experimentally in the conditions of this work. The scheme is further detailed in the text.

the scheme would involve only the native and I_2 states (Figure 8, right path).

The I_1 and I_2 species seem to retain the aggregation state induced by choline (Figure 8). Size-exclusion chromatography experiments in the presence of choline show I_1 and I_2 eluting as higher-molecular mass species than in the absence of ligand (Figures 4C and 4D). Moreover, the GdmCl-induced $I_1 \rightleftharpoons I_2$ transition monitored by fluorescence or $[\theta]_{226}$ displays the same energetics as those obtained for the unligated form (Figure 6A). This may not be expected if a coupled unfolding + monomerization process were involved. Moreover, despite the similarities in the CD spectra (Figure 2A), the fluorescence characteristics of I_2 depend on the presence of choline (Figure 2B), confirming that the conformational state of this species is choline-dependent.

It should be pointed out that although the I_1 and I_2 states accumulate in equilibrium on unfolding, their precise role in the kinetic folding of the C-LytA protein from the unfolded state (i.e. whether I_2 proceeds sequentially to I_1 , and this to N in the time course) remains to be established until CD- and fluorescence-monitored stopped-flow measurements are performed. On the other hand, the existence of a multistep process in the unfolding of C-LytA makes it necessary to revise the choice of the term 'domain' (e.g. 'choline-binding domain') to refer to this module, since the former expression should rather be reserved to represent a single co-operative structure.

As stated in the Introduction section, the C-LytA module is routinely used as an affinity tag for the single-step purification of fusion proteins ([15,17–19], and C-LYTAG® Purification System User's Manual from Biomedal, <http://www.biomedal.es>). We believe that some of the results presented in this paper would help in the design of new variants with an expanded landscape of applications. For example, it is well known that partly folded intermediates are very prone to aggregation [26]. Thus, deletion of the first 32 amino acids of C-LytA, which are probably unfolded in the I_1 state, may improve both the resistance to proteases and the solubility of the module and, therefore, of the corresponding fusion protein, without affecting its affinity for DEAE-based resins (Figure 5). Size reduction would also contribute to diminish possible steric interactions with the fused proteins. Furthermore, our efforts are currently aimed to identify fully the residual structure in the I_2 state, which seems capable of recognizing choline (Figure 2B). This structure shows an unusual stability against GdmCl denaturation, with a few similar examples in the literature [27], and might serve as a model for the design of robust β -hairpins that could be used as a drastically minimized version of C-LytA or as scaffolds for new functions.

In summary, we hypothesize that C-LytA denatures at 20°C by highly independent unfolding of ChBRs. In the absence of choline, the protein is partially unfolded in water, probably around its N-terminal part. Finally, the addition of saturating choline concentrations stabilizes the native state and reduces the number of intermediate species in the unfolding scheme. These results will presumably be valuable in the design of C-LytA variants with an enhanced biotechnological potential.

We thank A. Rodríguez, M. Gutiérrez, C. Fuster and J. Casanova for excellent technical assistance, J. Varela for the Edman analysis and A. Prieto for the MALDI-TOF experiment. We are grateful to Dr P. García and Dr J. L. García for supplying the RB791 [pCE17] strain, as well as for valuable discussions. We are indebted to Dr S. Padmanabhan for a critical reading of the manuscript. This work was funded by the Spanish Ministerio de Ciencia y Tecnología (grant BIO2000-0009-P4-C04) and the Escuela Valenciana de Estudios para la Salud (Generalidad Valenciana, Spain).

REFERENCES

- Mosser, J. L. and Tomasz, A. (1970) Choline-containing teichoic acid as a structural component of pneumococcal cell wall and its role in sensitivity to lysis by an autolytic enzyme. *J. Biol. Chem.* **245**, 287–298
- Tomasz, A. (1984) Building and breaking in the cell wall of bacteria. The role for autolysins. In *Microbial Cell Wall Synthesis and Autolysis* (Nombela, C., ed.), pp. 3–12. Elsevier, Amsterdam
- Berry, A. M. and Paton, J. C. (2000) Additive attenuation of virulence of *Streptococcus pneumoniae* by mutation of the genes encoding pneumolysin and other putative pneumococcal virulence proteins. *Infect. Immun.* **68**, 133–140
- Mitchell, T. J., Alexander, J. E., Morgan, P. J. and Andrew, P. W. (1997) Molecular analysis of virulence factors of *Streptococcus pneumoniae*. *Soc. Appl. Bacteriol. Symp. Ser.* **26**, 62S–71S
- Tuomanen, E. (1999) Molecular and cellular biology of pneumococcal infection. *Curr. Opin. Microbiol.* **2**, 35–39
- Díaz, E., López, R. and García, J. L. (1990) Chimeric phage-bacterial enzymes: a clue to the modular evolution of genes. *Proc. Natl. Acad. Sci. U.S.A.* **87**, 8125–8129
- Sánchez-Puelles, J. M., Sanz, J. M., García, J. L. and García, E. (1990) Cloning and expression of gene fragments encoding the choline-binding domain of pneumococcal murein hydrolases. *Gene* **89**, 69–75
- Sanz, J. M., Díaz, E. and García, J. L. (1992) Studies on the structure and function of the N-terminal domain of the pneumococcal murein hydrolases. *Mol. Microbiol.* **6**, 921–931
- López, R., García, E., García, P. and García, J. L. (1997) The pneumococcal cell wall degrading enzymes: a modular design to create new lysins? *Microb. Drug Resist.* **3**, 199–211
- Fernández-Tornero, C., López, R., García, E., Giménez-Gallego, G. and Romero, A. (2001) A novel solenoid fold in the cell wall anchoring domain of the pneumococcal virulence factor LytA. *Nat. Struct. Biol.* **8**, 1020–1024
- Fernández-Tornero, C., García, E., López, R., Giménez-Gallego, G. and Romero, A. (2002) Two new crystal forms of the choline-binding domain of the major pneumococcal autolysin: insights into the dynamics of the active homodimer. *J. Mol. Biol.* **321**, 163–173

- 12 Medrano, F. J., Gasset, M., López-Zúmel, C., Usobiaga, P., García, J. L. and Menéndez, M. (1996) Structural characterization of the unligated and choline-bound forms of the major pneumococcal autolysin LytA amidase. *J. Biol. Chem.* **271**, 29152–29161
- 13 Usobiaga, P., Medrano, F. J., Gasset, M., García, J. L., Saiz, J. L., Rivas, G., Laynez, J. and Menéndez, M. (1996) Structural organization of the major autolysin from *Streptococcus pneumoniae*. *J. Biol. Chem.* **271**, 6832–6838
- 14 Sanz, J. M., Lopez, R. and García, J. L. (1988) Structural requirements for 'conversion' of the pneumococcal amidase. A new single-step procedure for the purification of this autolysin. *FEBS Lett.* **232**, 308–312
- 15 Sánchez-Puelles, J. M., Sanz, J. M., García, J. L. and García, E. (1992) Immobilization and single-step purification of fusion proteins using DEAE-cellulose. *Eur. J. Biochem.* **203**, 153–159
- 16 Reference deleted
- 17 Caubin, J., Martin, H., Roa, A., Cosano, I., Pozuelo, M., de la Fuente, J. M., Sánchez-Puelles, J. M., Molina, M. and Nombela, C. (2001) Choline-binding domain as a novel affinity tag for purification of fusion proteins produced in *Pichia pastoris*. *Biotechnol. Bioeng.* **74**, 164–171
- 18 Ortega, S., García, J. L., Zazo, M., Varela, J., Muñoz-Willery, I., Cuevas, P. and Giménez-Gallego, G. (1992) Single-step purification on DEAE-sephacel of recombinant polypeptides produced in *Escherichia coli*. *Biotechnology* **10**, 795–798
- 19 Ruiz-Echevarría, M. J., Giménez-Gallego, G., Sabariego-Jareño, R. and Díaz-Orejas, R. (1995) KID, a small protein of the ParD stability system of plasmid R1, is an inhibitor of DNA replication acting at the initiation of DNA synthesis. *J. Mol. Biol.* **247**, 568–577
- 20 Greene, Jr, R. F. and Pace, C. N. (1974) Urea and guanidinium chloride denaturation of ribonuclease, lysozyme, α -chymotrypsin, and β -lactoglobulin. *J. Biol. Chem.* **249**, 5388–5393
- 21 Laemmli, U. K. (1970) Cleavage of structural proteins during the assembly of the head of bacteriophage T4. *Nature (London)* **227**, 680–685
- 22 Semisotnov, G. V., Rodionova, N. A., Razgulyaev, O. I., Uversky, V. N., Gripas, A. F. and Gilmanshin, R. I. (1991) Study of the 'molten globule' intermediate state in protein folding by a hydrophobic fluorescent probe. *Biopolymers* **31**, 119–128
- 23 Moczygemba, C., Guidry, J., Jones, K. L., Gomes, C. M., Teixeira, M. and Wittung-Stafshede, P. (2001) High stability of a ferredoxin from the hyperthermophilic archaeon *A. ambivalens*: involvement of electrostatic interactions and cofactors. *Protein Sci.* **10**, 1539–1548
- 24 Uversky, V. N. and Ptitsyn, O. B. (1994) 'Partly folded' state, a new equilibrium state of protein molecules: four-state guanidinium chloride-induced unfolding of beta-lactamase at low temperature. *Biochemistry* **33**, 2782–2791
- 25 Varea, J., Saiz, J. L., López-Zumel, C., Monterroso, B., Medrano, F. J., Arrondo, J. L. R., Iloro, I., Laynez, J., García, J. L. and Menéndez, M. (2000) Do sequence repeats play an equivalent role in the choline-binding module of pneumococcal LytA amidase? *J. Biol. Chem.* **275**, 26842–26855
- 26 Georgiou, G., Valax, P., Ostermeier, M. and Horowitz, P. M. (1994) Folding and aggregation of TEM β -lactamase: analogies with the formation of inclusion bodies in *Escherichia coli*. *Protein Sci.* **3**, 1953–1960
- 27 Chiaraluce, R., van der Oost, J., Lebbink, J. H. G., Kaper, T. and Consalvi, V. (2002) Persistence of tertiary structure in 7.9 M guanidinium chloride: the case of endo- β -1,3-glucanase from *Pyrococcus furiosus*. *Biochemistry* **41**, 14624–14632

Received 14 July 2004/1 December 2004; accepted 2 December 2004

Published as BJ Immediate Publication 2 December 2004, DOI 10.1042/BJ20041194